Electron channeling radiation experiments at very high electron bunch charges

R. A. Carrigan, Jr.*
Fermi National Accelerator Laboratory, Batavia, Illinois 60510, USA

J. Freudenberger,† S. Fritzler,‡ H. Genz, A. Richter, A. Ushakov,§ and A. Zilges
Institut für Kernphysik, Technische Universität Darmstadt, Schlossgartenstrasse 9, D-64289 Darmstadt, Germany

J. P. F. Sellschop‖
Schonland Centre, University of the Witwatersrand, 2050 Johannesburg, South Africa
(Received 6 August 2003; published 12 December 2003)

Plasmas offer the possibility of high acceleration gradients. An intriguing suggestion is to use the higher plasma densities possible in solids to get extremely high gradients. Although solid-state plasmas might produce high gradients they would pose daunting problems. Crystal channeling has been suggested as one mechanism to address these challenges. There is no experimental or theoretical guidance on channeling for intense electron beams. A high-density plasma in a crystal lattice could quench the channeling process. An experiment has been carried out at the Fermilab NICADD Photoinjector Laboratory to observe electron channeling radiation at high bunch charges. An electron beam with up to 8 nC per electron bunch was used to investigate the electron-crystal interaction. No evidence was found of quenching of channeling at charge densities two orders of magnitude larger than that in earlier experiments.

DOI: 10.1103/PhysRevA.68.062901 PACS number(s): 61.85.+p, 52.40.Mj, 61.80.Cb, 52.38.Hb

I. INTRODUCTION

Recently there has been interesting progress in studies of plasma acceleration in gas [1]. This has been due in part to the development of terawatt laser technology [2] about 15 years ago. Gas plasmas have already delivered gradients in the 1 GV/cm range [3,4], one to two thousand times higher than RF cavity gradients. Since accelerating gradients in a plasma are approximately given by $\sqrt{n}$ V/cm, where n is the plasma density, plasmas in solids can potentially deliver gradients 100 times higher than gas plasmas. For example, for $n=10^{22}/\mathrm{cm}^3$ in a solid, the gradient would be 100 GV/cm.

At the plasma densities required for acceleration there are severe material limitations. This has led to speculation about utilizing channeling [5] as an adjunct to solid-state plasma acceleration [6]. Channeling could mitigate the material problems and perhaps also introduce focusing to prevent beam blowup from multiple scattering. At the intensities needed for solid-state accelerators there will be significant channeling problems since the crystal lattice will be severely disturbed or the whole crystal may even be vaporized. As the bunch intensity rises energy loss and plasma generation with the concomitant rise in crystal disorder will cause degradation in channeling [7] so that channeling might be quenched.

If channeling is to be considered for solid-state acceleration, more information is needed on the character and limitations of channeling under extreme conditions. Although existing channeling theory can serve as a guide, no channeling studies have been done under the nonequilibrium conditions that couple intense electron-beam energy loss into a crystal. Understanding of the behavior of solids under the conditions required for acceleration is in its early stages [8]. These processes are complicated but have been investigated in connection with terawatt laser technology and pellet fusion.

A systematic study of channeling with increasing electron bunch charge was carried out at Darmstadt [9,10] using the superconducting Darmstadt electron linear accelerator S-DALINAC [11]. A planar channeling experiment has also been done at relatively high bunch charge at Stanford on the Stanford Mark III accelerator [12]. Both groups investigated channeling radiation from electron beams in the 5–30-MeV-energy region. The experiments, however, were some orders of magnitudes away from the plasma acceleration regime.

The new Fermilab A0 Photoinjector [13] produces a bunch intensity high enough to approach the plasma acceleration regime more closely. The injector uses a laser to photoproduce the intense, picosecond-long electron bunch. The accelerator typically operates with a kinetic energy of 14.4 MeV. An experiment has been carried out at the photoinjector to observe channeling radiation in the high bunch charge regime. The radiation was studied as a function of electron bunch intensity to investigate whether it quenched as the bunch intensity was increased. If crystal disorder reached the stage where channeling was quenched or extinguished the channeling radiation signal would diminish or disappear.

II. EXPERIMENT

Channeling radiation is straightforward to observe. Electrons moving along a crystal plane or axis oscillate and ra-

*Electronic address: Carrigan@fnal.gov
†Present address: Siemens Medical Solutions, Med RVV, P. O. Box 3260, D-91050 Erlangen, Germany; electronic address: joerg.freudenberger@siemens.com
‡Present address: Laboratoire d'Optique Appliquee–ENSTA, UMR 7639, CNRS, École Polytechnique, 91761 Palaiseau, France; electronic address: sven.fritzler@ensta.fr
§Present address: Institut für Angewandte Physik, Johann-Wolfgang-Goethe Universität Frankfurt, Robert-Mayer-Str. 12, D-60486 Frankfurt, Germany; electronic address: ushakov@iap.uni-frankfurt.de
‖Deceased.

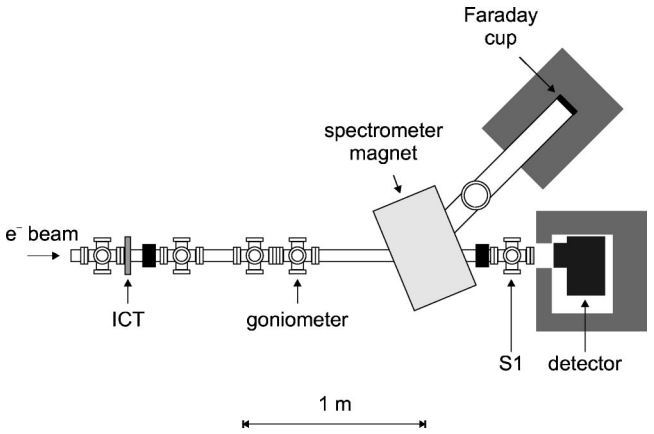

FIG. 1. A0 channeling radiation apparatus at Fermilab. The electron beam with bunch charges of up to 8 nC was provided by the photoinjector and typically had a kinetic energy of 14.4 MeV. The AberX and AberX-Lite detectors and the Faraday cup were surrounded by lead shields. Here ICT stands for integrating current transformer. The S1 port housed one of the view screens for AberX-Lite.

diate in much the same way as they do in a synchrotron. After the electron beam passes through the crystal it is deflected by a magnet. The undeflected channeling radiation is detected by an x-ray detector. In the relativistic regime the ''line energy'' of the radiation goes as $\gamma^{3/2}$ where γ is the Lorentz relativistic factor [14]. For electron beams at the A0 photoinjector the channeling x-ray energies are in the 10-100 keV range. Channeling x rays were separated from other sources such as bremsstrahlung by scanning the crystal through the characteristic channeling angular distribution that has a width related to the Lindhard critical angle. The expected channeling radiation x-ray yield per electron for Si is on the order of 10^{-4}. For the experiment at A0 there were characteristically 5×10^{10} electrons in a bunch so that there were of the order 5×10^{6} channeling x rays per bunch. These were concentrated in a cone that had an angular half-width of $1/\gamma$ or 30 mrad. In a picosecond-long pulse 10^5 photons struck a 125-mm^2 detector 1.47 m downstream of the crystal.

Figure 1 shows a schematic drawing of the Fermilab channeling radiation apparatus at A0. This setup consisted of a crystal mounted in a remotely controlled goniometer, a spectrometer magnet to deflect the electron beam, and an x-ray detector system. Beam current was measured with an integrating current transformer (ICT) and a Faraday cup. The 20-μm thick, 25-mm diameter Si crystal was obtained from Virginia Semiconductor. It was mounted with the $\langle 100\rangle$ axis along the beam line and the (110) planes in the horizontal and vertical directions, respectively. The goniometer had two angular degrees of freedom, Θ_x and Θ_y, i.e., the crystals could be rotated around a horizontal and a vertical axis perpendicular to the beam axis, respectively. The goniometer design was dictated by the requirements of the photoinjector dust-free, very high vacuum system.

A. Photoinjector beam

The A0 photoinjector normalized rms beam emittance with 6 nC/bunch was typically $\varepsilon_n = 12$ mm mrad for the experiment [15]. This was in line with simulations using the program HOMDYN [16]. The emittance depends on bunch charge and is proportional to bunch charge plus a small intrinsic part. The beam-spot size at the crystal was typically 0.5 mm (σ) so that the corresponding angular divergence was 0.7 mrad at 6 nC. This is somewhat smaller than the axial channeling critical angle which is about $\psi_c = 2.4$ mrad for the Si $\langle 100\rangle$ axis at A0 energies obtained from extrapolating Darmstadt data [17] taken at 6.7 MeV. The bunch length for a 5-nC bunch measured using a streak camera was typically $\sigma_t = 7$ ps.

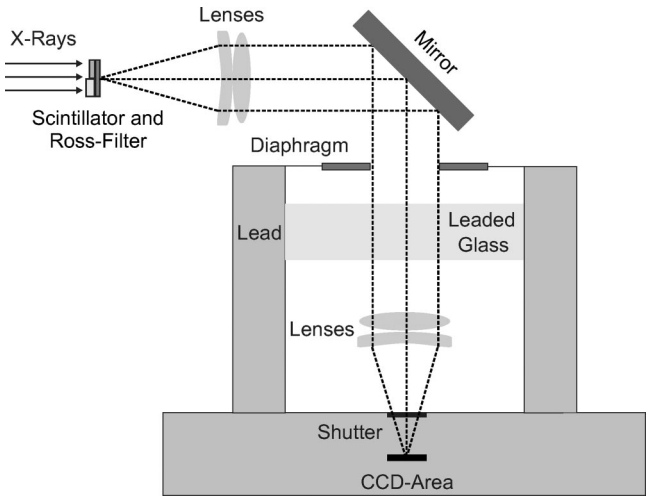

FIG. 2. AberX CCD x-ray detector system. After passing the Ross filter the x rays were converted by means of a terbium-doped gadoliniumoxisulfide foil into visible light with a wavelength of 545 nm that was focused onto a CCD camera. Using the nine different absorber foils of the Ross filter system enabled the detection of x rays from 9 to 26 keV with an energy resolution of 1–3 keV.

B. X-ray detectors

Conventional single x-ray detectors do not work in the extremely high x-ray flux environment of the A0 photoinjector. Instead two special x-ray detector systems were used. One employed an absorption-based, energy-resolved x-ray detector (AberX) that used a Ross filter [18] and a lens-coupled scintillating screen–charge-coupled device (CCD) system. This detector was developed by Freudenberger [19] to study its feasibility for mammography. The Ross filter technique takes advantage of the *K* edge absorption of x rays by thin metallic foils. An A0 channeling radiation result obtained with that detector has already been discussed [20]. The second scheme, the so-called AberX-Lite system, replaced the CCD screen with one or two photomultipliers to achieve a faster response time.

1. The AberX detector

The AberX detector system is shown in Fig. 2. X rays were detected in AberX by means of a thin fluorescent x-ray foil or scintillator that converted the incoming x rays into visible light. The image of this foil was then focused on to a CCD camera by an optical lens system. The CCD area was surrounded by lead shielding as well as lead glass that pro-

tected against scattered x rays. Variable exposure times could be selected with a mechanical shutter. The CCD readout was carried out at a low pixel rate of 100 kHz for optimum noise suppression.

The 40-μm thick fluorescent x-ray converter foil of Terbium-doped gadoliniumoxisulfide Gd_2O_2S:Tb has the largest conversion rate known for photons. For the foil about 19% of the energy of the absorbed x rays is emitted in the form of photons with an average energy of 2.2 eV corresponding to a wavelength of 545 nm. This resulted in an energy dependent photon conversion rate, for the foil, of

$$\xi_F(E)=\frac{N_p(E)}{N(E)}=0.19(1-\tau_{Gd})(E/2.2), \tag{1}$$

where $N_p(E)$ and $N(E)$ represent the emitted photon yield and the incident x-ray flux, respectively, τ_{Gd} denotes the x-ray transmission probability of the Gd_2O_2S:Tb foil and E the x-ray energy in eV. A symmetric lens system with a numerical aperture of $X_{\mathrm{NA}}=0.25$ mapped the intensity distribution in full scale to a front-illuminated, low noise, slow scan CCD camera ($X_{\mathrm{NA}}=D/2f$, where D denotes the effective diameter of the lens and f its focal length). The CCD system utilized a screen with an array of 512×512 pixels. Each pixel was of size 24 μm$\times$24 μm. The fraction of the light per solid angle collected by the CCD lens system was

$$\xi_L=\frac{1}{2}\left(1-\frac{1}{\sqrt{1+X_{\mathrm{NA}}^2}}\right). \tag{2}$$

The quantum efficiency of the CCD camera was $\xi_{CCD}=0.28$ at 550 nm. The total efficiency of the AberX detector depended on the properties of the fluorescent screen, the light transport, and the quantum efficiency of the CCD camera. The overall detector response was

$$\xi_A(E)=\xi_F\xi_L\xi_{CCD}, \tag{3}$$

so that $\xi_A=950\times0.0149\times0.28=4$ which meant that four photons emitted by the screen per incoming x ray of 25 keV were registered by the CCD.

The detector array described so far was sensitive only with respect to the position of the x ray hitting the scintillator foil. A Ross filter was mounted in front of the AberX detector to obtain x-ray energy information and thereby determine the spectral distribution of the channeling x rays. The filter consisted of nine different absorber materials of different thicknesses. The principle of the filter is shown in Fig. 3. The transmission of x rays through the 25-μm niobium foil and the 35-μm zirconium foil differed only in the range between the K-absorption edges at 18.00 and 18.99 keV, respectively. The difference in counting rate between the pixels covered by Nb and Zr yielded the x-ray intensity in that energy window. The selection of the nine different absorber foils thus enabled the detection of x rays from 9 to 26 keV with an energy resolution of 1–3 keV in the energy region of the expected channeling features of this experiment.

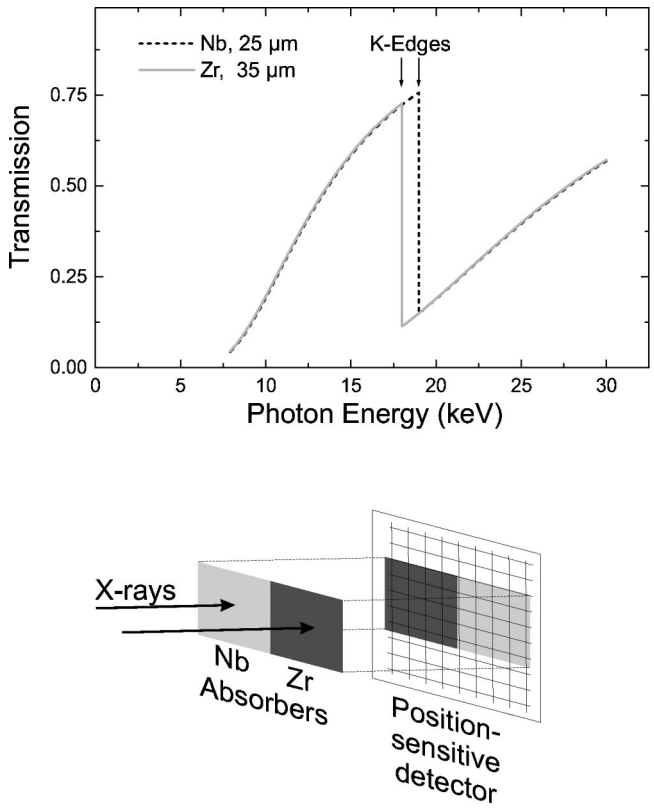

FIG. 3. Principle of the Ross filter. Upper panel, adjacent Z transmission curves; and lower panel, detection by the CCD camera. Since the transmission curves differ only between the K-absorption edges the difference in counting rate between the pixels covered by the two foils yields the x-ray intensity in the energy region between the K-absorption edges. The selection of different materials and thicknesses thus enables the system to act as an x-ray spectrometer.

The general system response was calibrated by comparing the measured x-ray response from a filtered 26-keV x-ray tube. The energy response and relative yield were in good agreement.

2. The AberX-Lite detector

The second approach employed x-ray detectors made with calcium tungstate scintillation films monitored by photomultipliers. Two versions of AberX-Lite were used at different times. One was positioned near the location of AberX (1.47 m downstream of the crystal). This version used two photomultipliers behind Ross filter foil pairs mounted on a rotatable wheel. A later version using a single phototube without a Ross filter was located 1.01 m downstream of the crystal inside the accelerator vacuum pipe at the S1 vacuum port (Fig. 1). For most of the measurements reported here, the Ross filter was not used so the detectors responded to all of the channeling radiation x rays up to several hundred keV. Because of the nanosecond response, the photomultiplier system had the advantage of bunch-to-bunch readout of the x-rays making it easier to measure dark current and subtract it. It is for this reason that this detector was used to collect most of the data in the present work.

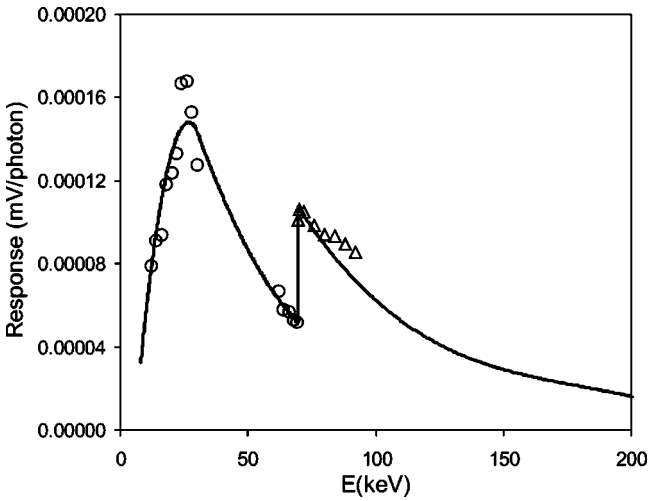

FIG. 4. Calibrated response of the AberX-Lite detector. The calibration was carried out using monochromatic x rays with variable energy at the Argonne Advanced Photon Source (APS) relative to a calibrated ion chamber. The solid line represents the results of a model fit to the points indicated by circles. The triangles above the W *K* edge were not used in the fit.

The AberX-Lite detector system was calibrated in two separate ways. In one, the detector system was placed in a monoenergetic x-ray beam with variable energy at the Argonne Advanced Photon Source (APS). The x-ray flux was measured with a calibrated ion chamber. The detector calibration extended over a 12–92 keV region which included the tungsten *K* edge. This gave the absolute response of the detector as a function of energy and the calibration of the Ross absorber system. The detector response is shown in Fig. 4 as a function of x-ray energy in millivolts per x-ray photon. It is consistent with the detector scintillator thickness and the expected light yield of calcium tungstate up to the W *K* edge at 69.5 keV. Beyond that the experimental response was 0.6 of the theoretical response, possibly due to something like optical photon leakage before conversion. The response of the detector to x rays from axial channeling was calculated by integrating the measured detector response times the channeling radiation spectrum, that is,

$$S_L = F \int_0^{E_m} N(E)\xi_C(E)dE, \tag{4}$$

where S_L is the AberX-Lite yield, F is a constant determined by the calibration, $N(E)$ is the channeling radiation spectrum, and $\xi_C(E)$ is the fit to the calibrated response. The channeling radiation distribution, $N(E)$, was determined from the 6.7-MeV Si $\langle 111 \rangle$ data of Genz *et al.* [21] scaled to 14.4 MeV assuming the channeling radiation lines scaled as $\gamma^{3/2}$. Kumakhov and Wedell [14] suggest that the channeling radiation lines should scale as $1/d$ where d is the interatomic distance along the string. For Si$\langle 100 \rangle$/Si$\langle 111 \rangle$ this gives 1.29. The scaled 6.7-MeV Si$\langle 111 \rangle$ data was multiplied accordingly. The 16.9-MeV diamond $\langle 100 \rangle$ data from Klein *et al.* [22] scaled to 14.4 MeV matches the 6.7-MeV Si$\langle 111 \rangle$ scaled data.

In the second method the calibration was determined by integrating the x-ray yield over the bremsstrahlung spectrum for a random (nonchanneling) orientation of the crystal. While the two calibrations were consistent the bremsstrahlung technique was less accurate because nonbremsstrahlung contributions such as background were a significant part of the random signal. Only results based on the Argonne APS calibration are thus presented here.

Signal information from calcium tungstate was collected using a digital oscilloscope. The scope integrated over the $CaWO_4$ pulse, collected data from the integrating current transformer (ICT in Fig. 1), and normalized the ICT signal to get the charge. The scintillation light time distribution for the $CaWO_4$ has two time components; a short one with a time constant of 4 μs and a stronger one with an 8 μs decay. The A0 photoinjector bunch train consisted of a series of laser-driven pulses, each several picoseconds long, separated by 1 or 2-μs intervals. There was a background of dark current pulses coming at the 1.3 GHz frequency of the RF. Typically the amplitude of a dark current pulse was $10^{-4}-10^{-5}$ of the amplitude of a laser-driven pulse. The relative amplitudes of the two sets of pulses could be controlled by changing the laser-pulse intensity and the amplitude of the RF on the photoinjector RF gun. Since the principal aim of the experiment was to observe the channeling signal as a function of bunch charge it was desirable to operate over as wide a range of bunch charges as possible. This was done in two ways—by changing the laser intensity and by measuring the dark current yields. For the laser case care was taken to suppress the dark current by lowering the voltage of the RF gun and then subtracting the residual by measuring the dark current just before the laser pulse and with no laser pulse. Typically measurements were made on the first laser pulse in a train and averaged over 10 cycles (the A0 photoinjector operated at 1 Hz during the experiment).

III. ANALYSIS

Data were taken by first scanning the goniometer through Θ_x and Θ_y to find a plane, an axis, or a random orientation of the crystal. Most of the random background was due to bremsstrahlung in the crystal. The ''no crystal'' background was typically 17% of the yield on axis since even a small electron or x-ray halo was amplified significantly because the crystal holder was more than 100 times the thickness of the crystal. Figure 5 shows typical scans through several planes (left panel) and the $\langle 100 \rangle$ axis (right panel) using AberX-Lite. In the axial scan the crystal moved from the axis along a (110) plane because these planes were oriented in the horizontal and vertical directions.

A. AberX-Lite analysis

For AberX-Lite the axial peak (Fig. 5 right panel) was fitted with two colocated Gaussians to account for the tilted planar portion. One of the fitting Gaussians had a width (σ) of $\psi_{am}=4$ mrad while the second one had an amplitude of 0.75 of the first and a width of 12 mrad. These parameters were determined by fitting a number of scans with these

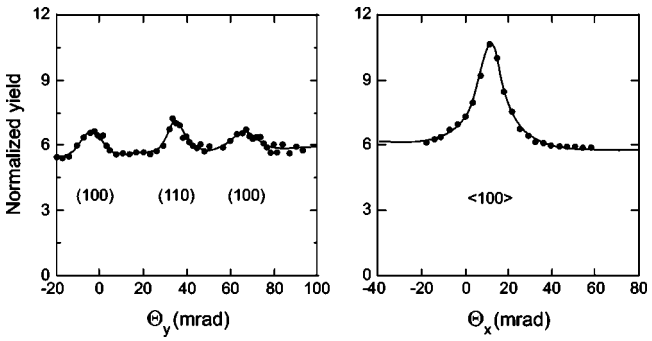

FIG. 5. X-ray yields for planar (left panel) and axial (right panel) scans obtained from a Si crystal in the 14.4-MeV electron beam. The quantities Θ_x and Θ_y describe the rotation of the crystal around a horizontal and a vertical axis perpendicular to the beam axis, respectively. The yields were measured using the AberX-Lite detector. The solid line fitted to the axial spectrum results from a double Gaussian fitting function as explained in the text.

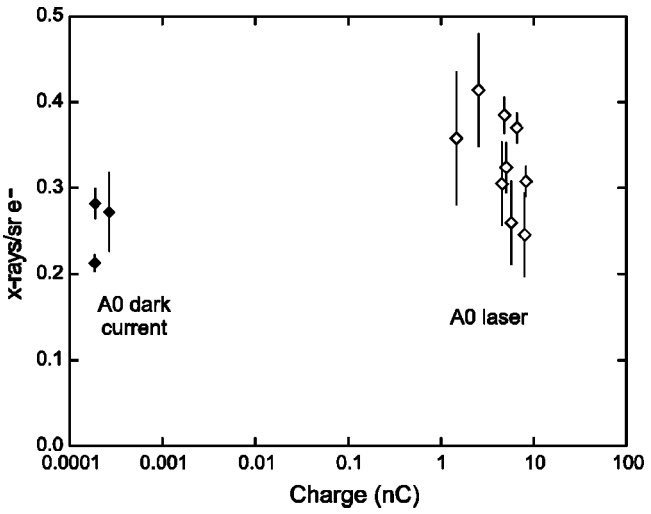

FIG. 6. Axial channeling radiation yield (x-rays/sr e^-) as a function of bunch charge at A0 obtained with the AberX-Lite detector. The open diamonds represent the data obtained with the rf gun laser on, that is, from channeling radiation produced by laser-induced photoelectrons. The filled diamonds show the data points resulting from the exposure of the crystal to electrons due to the rf gun dark current only.

quantities as free parameters. The 4-mrad width of the principal Gaussian in the axial scan curve is consistent with the axial critical angle convoluted with an error distribution of 3.2 mrad (σ). This resolution spread arose from contributions from beam divergence, possible crystal distortions, goniometer vibration, and multiple scattering. The ratio of the widths of the (100) and the (110) planes were consistent with the fact that the 45° planes were scanned diagonally. The ratio of planar heights to axial height is consistent with earlier experiments. A fixed dilution multiplier of $\psi_{am}/\psi_c = 1.66$ was applied to the 4-mrad Gaussian to account for dilution due to the 3.2-mrad error distribution. A second multiplicative factor accounted for the fact that the actual axial signal was larger than the sum of the two Gaussians because the fit included the effect of the plane in the scan direction in the random portion. That is to say, the actual height above the random background was larger than just the sum of the two Gaussians because the scan continued to follow a plane which contributed to the putative sloping background fit. The averaged multiplicative correction factor for this effect was 1.23. A negative, charge-dependent correction was incorporated to account for the dark current contribution to the axial peak height.

Contributions to the errors arose from the deviations of the fit to the scan curve including the axial line and background portion, the error on the dark current yield determination, and the deviation of the charge measurement. Typically for bunch charges greater than 5 nC the contributions for the peak fit, the charge measurement, and the dark current were comparable. However, for smaller charges the dark current error became the dominant contribution so that the error bars are substantially larger at small charge Q. Below 1 nC it was impractical to make a useful measurement because of this effect. Those points have been omitted. Obviously no dark current corrections were required for the dark current measurements.

Systematic errors (not shown in the figures) arose from uncertainty concerning the crystal thickness, uncertainties in approaches to the Argonne detector normalization, and uncertainties about how to treat the impact of resolution spreading on the axial peak. None of these was strongly dependent on the bunch charge. No correction was made for x-ray adsorption in the crystal since it was small when integrated over the x-ray energy distribution.

Figure 6 shows the axial x-ray yield per steradian electron at $T = 14.4$ MeV as a function of bunch charge (nC) for the A0 AberX-Lite axial measurements. The figure includes both laser (open diamonds) and dark current (filled diamonds) measurements. These results are for the total x-ray yield integrated over x-ray energy. These data illustrate the behavior over a range of bunch charges with the same material and orientation. Within the error bars the yield is essentially flat over five decades.

B. AberX analysis

The intensity through the AberX system was determined by measuring the image density behind each of the Ross filter elements. The signal S_{Ai}, the number of optical photons/x ray for the ith filter, was then

$$S_{Ai} = \int_0^{E_m} N(E)\tau_i(E)\xi_A(E)dE, \tag{5}$$

where $N(E)$ is the channeling radiation spectrum (the number of x rays per unit x-ray energy for the exposure), $\tau_i(E)$ is the transmission of the ith Ross filter element, and $\xi_A(E)$ is the light yield from Eq. (3). The transmission difference between a set of K edges is given by

$$\Delta S_A \sim N(\overline{E})\xi_A(\overline{E}) \int_{E_{K,i-1}}^{E_{K,i}} [\tau_i(E) - \tau_{i-1}(E)]dE. \tag{6}$$

The x-ray yield is then

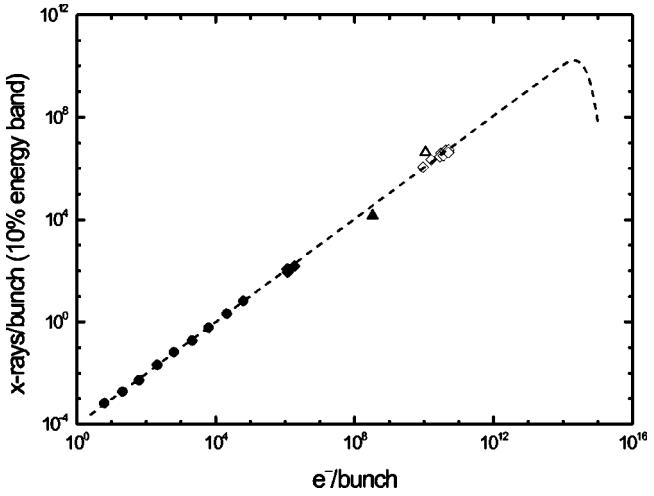

FIG. 7. Channeling radiation yield (x-rays/bunch in a 10% band) over a 12-decade span of bunch charge. The present data are represented for the AberX-Lite detector by open and filled diamonds obtained for axial channeling from Si with the laser on and with dark current, respectively, and for the AberX detector as indicated by the open triangle for planar channeling. The filled circles [9] result from an earlier measurement of axial channeling in a diamond crystal with electrons of 5.4 MeV and the filled triangle [23] from planar channeling in a Si crystal at 30 MeV. All points have been scaled to $T=5.4$ MeV.

$$N(\overline{E}) \sim \frac{\Delta S_A}{\xi_A(\overline{E}) T_{i,i-1}}, \tag{7}$$

where

$$T_{i,i-1} = \int_{E_{K,i-1}}^{E_{K,i}} [\tau_i(E) - \tau_{i-1}(E)] dE. \tag{8}$$

For the highest point in the AberX channeling radiation spectrum at $E=(25\pm0.5)$ keV Eq. (7) gives $N(\overline{E})=(4.2\pm0.8)\times10^{-6}$ photons/bunch. The charge of the electron bunch amounted to 1.76 ± 0.1 nC so that the number of electrons per bunch was $(1.10\pm0.06)\times10^{10}e^-$/bunch. The error quoted is caused by the uncertainties of the light efficiency of the AberX converter screen, the CCD efficiency, and the solid angle.

IV. RESULTS

Figure 7 illustrates the x-ray yield per bunch integrated over solid angle as a function of electrons/bunch for a 10% energy band around the peak of the channeling x-ray spectrum. Both the A0 measurements and earlier high bunch charge experiments at Darmstadt and Stanford are included. The logarithmic plot illustrates the very wide dynamic range in bunch charge spanned by the experiments. The x-ray yield increases linearly over more than 10 decades. The A0 measurements have extended the bunch charge reach by more than a factor of 100. The filled circles [9] are Darmstadt data for a 50-μm diamond crystal taken at 5.4 MeV with the beam aligned on the $\langle 110 \rangle$ axis. The filled triangle is a Stanford Si (110) planar point [23] taken at 30 MeV. (In fact, the theoretical value for the 1-0 transition was used since there was no experimental measurement for that line. However the rest of the experimental and theoretical spectrum was in fair agreement.) The Stanford crystal was 15-μm thick. The yield has been scaled to the 5.4-MeV Darmstadt points by multiplying by the ratio of $\gamma^{1/2}$ for the two energies to account for the lower channeling radiation yield integrated over solid angle at 5.4 MeV. The Stanford yield was also multiplied by an appropriate solid angle factor. The yield over a 10% energy band was found by integrating the Stanford data. No correction was made to take account of the fact that the Stanford measurement was for planar Si rather than axial diamond. The open diamonds are the A0 AberX-Lite laser points for Si $\langle 100 \rangle$. They have been scaled from 14.4 MeV to 5.4 MeV using $\gamma^{1/2}$ and divided by a factor of 13.5 to give the yield in a 10% energy band rather than the total x-ray yield. The filled diamonds are the dark current measurements for A0 AberX-Lite treated in the same way. The planar A0 result using the AberX detector is shown as an open triangle. It has also been energy scaled to the Darmstadt 5.4-MeV results. No correction was made to take account of the fact that the A0 measurements were for different orientations and Si rather than diamond.

Differences of order 2 are expected between the various datasets because of different materials, orientations, and thicknesses. In addition, the various techniques are quite different. In particular, adjusting the higher beam energy points from A0 and Stanford to the Darmstadt 10% energy band requires extrapolations that are susceptible to assumptions about the spectral distributions. The dashed line is a fit to the original Darmstadt data, which are extrapolated and thus schematically illustrate how the channeling radiation yield might quench with increasing bunch charge. Even with the differences in techniques, orientations, thicknesses, and materials the axial results are flat within a factor of 2 over 10 decades. No evidence has been found of quenching of channeling at charge densities several orders of magnitude larger than that in earlier experiments.

This experiment has reached bunch charges of up to 8 nC in a beam-spot size with a σ of 0.5 mm and a pulse length of $\sigma=7$ ps. This corresponds to a current on the order of 1000 A and a current density of 10^5 A/cm^2. The effective power density deposited in the crystal at A0 is typically 10^{12} W/cm^3. Achieving a 1-GeV/cm gradient could require drive beam power densities in the range of 10^{19}–10^{21} W/cm^3 so that the experiment is still a factor of 10^7–10^9 away from where significant channeling acceleration could happen. Parenthetically, for an exposure of roughly 3×10^{17} electrons/mm^2, there was no sign of spotting or crystal crazing visible to the naked eye or deterioration of the channeling radiation signal over the course of the experiment. The earlier Stanford work [23] found no damage for an exposure of 0.5×10^{17} electrons/mm^2.

V. OUTLOOK FOR SOLID-STATE PLASMA ACCELERATION

Several approaches to solid-state plasma acceleration have been discussed. One, particle beam wake field accelera-

tion uses a particle beam as a plasma driver. A laser beam can also be used to drive a plasma. Another approach is to use a side injected laser to avoid problems with pump depletion and particle dephasing [24]. Pump depletion is particularly troubling for the high plasma densities in solids. Approaches using laser beams are limited by the optical absorption depth for materials such as Si and Ge as well as surface reflection.

As noted above, the A0 experiment is still far from the regime where significant solid-state acceleration might occur. At A0 bunch compression can be used to reduce the bunch length to about 1 ps and the spot size might be reduced by a factor of 2 so that it may be possible to go one order of magnitude further toward the conditions required for plasma acceleration. A major problem for studying solid-state acceleration is the bunch length. Getting into the plasma regime requires bunch lengths of the order of 10 fs. An approach to higher bunch charge densities is to go to a higher-energy accelerator such as SLAC. There one might obtain beams with transverse sizes on the order of 5 μm and bunch lengths of 50 fs [25]. This would increase the effective power densities by 10^5-10^6 over the A0 result and approach much closer to the solid-state plasma regime. However a very different experimental technique would be required. Another approach would be to use a fairly modest electron beam coupled with extremely intense laser illumination.

Although the A0 experiment reported here was far from the plasma regime in both current and pulse length, an initial search for plasma acceleration at A0 could be performed by assuming that the beam itself would generate a plasma. The putative wake field could affect the tail end of the bunch so that it gained or lost energy. This has been the approach employed by the gas plasma experiment already carried out at A0 [26]. This could be observed by using the spectrometer magnet to look for a changing shape of the momentum distribution after the spectrometer with higher bunch intensities and with the crystal aligned for channeling or a random direction. The rms multiple-scattering angle for the crystal produces a projected multiple-scattering angle of 12 mrad. This is equivalent to a momentum resolution of 0.6 MeV/c. A plasma density of about 10^{17} e^-/cm^3 would give a gradient of 0.3 GV/cm to give 0.6 MeV in the 20-μm crystal. This could be achieved with a side coupled laser with an intensity of 3×10^{15} W/cm^2. The A0 laser can reach 10^8–10^9 W/cm^2 for a 1.8-ps pulse. Thus at present it is not possible to reach into the acceleration regime at A0 with the existing A0 laser.

ACKNOWLEDGMENTS

The help of H. Edwards, W. Muranyi, J. Santucci (Fermilab), D. Haeffner, P. Lee, A. Mashayekhi, A. McPherson (Argonne), W. Hartung (Michigan State), R. Noble (Stanford), J. Carneiro (DESY), M. Fitch (Johns Hopkins), and N. Barov (NIU) is gratefully acknowledged. We thank Dr. Sergiy Khodyachykh for bringing the manuscript into its final form. The work was operated by Universities Research Association, Inc. under Contract No. DE-AC02-76CH0300 with the U.S. Department of Energy. This work was also supported by BMBF under Contract No. 06DA915I and by DFG Project No. GK410.

[1] C. Joshi, in *Advanced Accelerator Concepts*, edited by Patrick L. Colestock and Sandra Kelley, AIP Conf. Proc. 569 (AIP, Melville, NY, 2001), p. 85.

[2] See, for example, *Advanced Accelerator Concepts*, edited by Swapan Chattopadhyay, Julie McCullough, and Per Dahl, AIP Conf. Proc. 398 (AIP, Woodbury, NY, 1997).

[3] D. Gordon, K.C. Tzeng, C.E. Clayton, A.E. Dangor, V. Malka, K.A. Marsh, A. Modena, W.B. Mori, P. Muggli, Z. Najmudin, D. Neely, C. Danson, and C. Joshi, Phys. Rev. Lett. **80**, 2133 (1998).

[4] M.J. Hooga, C.E. Clayton, C. Huang, P. Muggli, S. Wang, B.E. Blue, D. Walz, K.A. Marsh, C.L. O'Connell, S. Lee, R. Iverson, F.-J. Decker, P. Raimondi, W.B. Mori, T.C. Katsouleas, C. Joshi, and R.H. Siemann, Phys. Rev. Lett. **90**, 205002 (2003).

[5] For recent summaries of channeling, see H. Andersen, R. Carrigan, and E. Uggerhoj, Nucl. Instrum. Methods Phys. Res. B **119** (1996); R.A. Carrigan, Jr., in *Handbook of Accelerator Physics and Engineering*, edited by A. Chao and M. Tigner (World Scientific, Singapore, 2002), p. 499.

[6] P. Chen and R.J. Noble, in *Relativistic Channeling*, edited by R.A. Carrigan, Jr. and J.A. Ellison (Plenum, New York, 1987), p. 517; P. Chen and R. Noble, in *Advanced Accelerator Concepts*, edited by Swapan Chattopadhyay, Julie McCullough, and Per Dahl, AIP Conf. Proc. 398 (AIP, Woodbury, NY, 1997), p. 273.

[7] R.A. Carrigan, Jr., in *Advanced Accelerator Concepts*, edited by Swapan Chattopadhyay, Julie McCullough, and Per Dahl, AIP Conf. Proc. 398 (AIP, Woodbury, NY, 1997), p. 146.

[8] J. Davis, R. Clark, and J. Giuliani, Laser Part. Beams **13**, 3 (1995).

[9] W. Lotz, H. Genz, P. Hoffmann, U. Nething, A. Richter, A. Weickenmeier, H. Kohl, W. Knüpfer, and J.P.F. Sellschop, Nucl. Instrum. Methods Phys. Res. B **48**, 256 (1990).

[10] H. Genz, L. Groening, P. Hoffmann-Stascheck, A. Richter, M. Höfer, J. Hormes, U. Nething, J.P.F. Sellschop, C. Toepffer, and M. Weber, Phys. Rev. B **53**, 8922 (1996).

[11] A. Richter, Physikalische Blätter **54**, 31 (1998).

[12] C.K. Gary, A.S. Fisher, R.H. Pantell, J. Harries, and M.A. Piestrup, Nucl. Instrum. Methods Phys. Res. B **51**, 458 (1990).

[13] J.-P. Carneiro *et al.*, in *Proceedings of the 1999 Particle Accelerator Conference*, edited by A. Luccio and W. MacKay (IEEE Publishing, Piscataway, NJ, 1999), p. 2027–2029.

[14] See, for example, M. Kumakhov and R. Wedell, *Radiation of Relativistic Light Particles during Interactions with Single Crystals* (Spektrum, Heidelberg, 1991).

[15] J.-P. Carneiro, Ph.D thesis, Université de Paris XI, UFR Scientifique D'Orsay, 2001 (unpublished).

[16] M. Ferrario *et al.*, Part. Accel. **52**, 1 (1996).

[17] W. Lotz, Ph.D. thesis, Technische Hochschule Darmstadt, D17, 1990 (unpublished).

[18] See, for example, P.A. Ross, Phys. Rev. **28**, 425 (1926); I.V. Khutoretsky, Rev. Sci. Instrum. **66**, 773 (1995).
[19] J. Freudenberger, Ph.D. thesis, Technische Universität Darmstadt, D17, 1999 (unpublished).
[20] H. Genz, in *Electron-Photon Interaction in Dense Media*, edited by H. Wiedemann (Kluwer Academic, Dordrecht, The Netherlands, 2001), p. 217.
[21] H. Genz, H.-D. Gräf, P. Hoffmann, W. Lotz, U. Nething, A. Richter, H. Kohl, A Weickenmeier, W. Knüpfer, and J.P.F. Sellschop, Appl. Phys. Lett. **57**, 2956 (1990).
[22] R.K. Klein, J.O. Kephart, R.H. Pantell, H. Park, B.L. Berman, R.L. Swent, S. Datz, and R.W. Fearick, Phys. Rev. B **31**, 68 (1985).
[23] C.K. Gary, A.S. Fisher, R.H. Pantell, J. Harries, and M.A. Piestrup, Phys. Rev. B **42**, 7 (1990).
[24] T. Katsouleas, J.M. Dawson, D. Sultana, and Y.T. Yan, IEEE Trans. Nucl. Sci. **NS-32**, 3554 (1985).
[25] P. Chen (private communication).
[26] N. Barov, K. Bishofberger, J.B. Rosenzweig, J.P. Carneiro, P. Colestock, H. Edwards, M.J. Fitch, W. Hartung, and J. Santucci, in Proceedings of Particle Accelerator Conference (unpublished).